

# **Parameter-dependent behavior of articular cartilage: 3D mechano-electrochemical computational model**

Sara Manzano<sup>1,2,3</sup>, Manuel Doblaré<sup>1,2,3</sup> and Mohamed Hamdy Doweidar<sup>1,2,3\*</sup>

<sup>1</sup>Group of Structural Mechanics and Materials Modelling (GEMM), Aragón Institute of Engineering Research (I3A), University of Zaragoza, Spain.

<sup>2</sup>Mechanical Engineering Department, School of Engineering and Architecture (EINA), University of Zaragoza, Spain.

<sup>3</sup>Biomedical Research Networking Center in Bioengineering, Biomaterials and Nanomedicine (CIBER -BBN), Spain.

Corresponding author: \*Mohamed Hamdy Doweidar

Email: [mohamed@unizar.es](mailto:mohamed@unizar.es)

Mechanical Engineering Department, School of Engineering and Architecture (EINA), University of Zaragoza, María de Luna s/n, Betancourt Building, 50018 Zaragoza, SPAIN. Phone: +34 876555210

## **Abstract**

**Background and Objective:** Changes in mechano-electrochemical properties of articular cartilage play an essential role in the majority of cartilage diseases. Despite of this importance, the specific effect of each parameter into tissue behavior remains still obscure. Parametric computational modeling of cartilage can provide some insights into this matter, specifically the study of mechano-electrochemical properties variation and their correlation with tissue swelling, water and ion fluxes. Thus, the aim of this study is to evaluate the influence of the main mechanical and electrochemical parameters on the determination of articular cartilage behavior by a parametric analysis through a 3D finite element model. **Methods:** For this purpose, a previous 3D mechano-electrochemical model, developed by the same authors, of articular cartilage behavior has been used. Young's modulus, Poisson coefficient, ion diffusivities and ion activity coefficients variations have been analyzed and quantified through monitoring tissue simulated response. **Results:** Simulation results show how Young's modulus and Poisson coefficient control tissue behavior rather than electrochemical properties. Meanwhile, ion diffusivity and ion activity coefficients appear to be vital in controlling velocity of incoming and outgoing fluxes. **Conclusions:** This parametric study establishes a basic guide when defining the main properties that are essential to be included into computational modeling of articular cartilage providing a helpful tool in tissue simulations.

**Keywords:** Parametric analysis, articular cartilage, mechano-electrochemical model, cartilage Young's modulus, ion diffusivity, ion activity coefficient.

## **1 Introduction**

Articular cartilage plays a vital role in the function of diarthrodial joints (Boschetti et al. 2004). The initial event that triggers pathological process of cartilage degeneration is still unknown (Wilson et al. 2005). Hence, to investigate the initiation of cartilage diseases, most important parameters that control its behavior should be determined. So far, the common method to accomplish that, are specific experimental assays (Pearle et al. 2005; Albro et al. 2009; Virén et al. 2009). However, these techniques require high costs and elevate time consuming. Besides, experimental approaches limit the study of parameters in an individual manner. To solve these problems, in the last decade, it has emerged the use of computational models to simulate cartilage behaviour (Landinez-Parra et al. 2011; Seifzadeh et al. 2012) as well as materials mimicking cartilage (Manzano et al. 2014; Krishnan Namboori et al. 2013). Therein, the finite element method is the most used (Soulhat et al. 1999; Smith et al., 2013). In the literature many material models for articular cartilage can be found. These models range from relatively simple, including the biphasic nature of the tissue (Higginson et al., 1976; Chen et al. 1997), to models that include descriptions of all major individual components of the cartilage (Mow and Guo 2002; Ateshian et al. 2013; Manzano et al. 2014a; Manzano et al. 2014b; Sun et al. 2004). However, the main parameters to consider in these simulations remain still obscure since the requirements of a material model are highly dependent on the particular question under research. In general, the more features of the composition and structure of articular cartilage are included, the larger the number of material parameters that must be determined, and the more computationally expensive the model becomes. Hence, we should always try to use

the simplest model with the lowest number of tissue properties to obtain the required data but without compromising the predictive capacity of the computational model.

The present parametric study faces important questions like: i) is the weakening of collagen matrix enough for tissue to swell or it is required to consider the proteoglycans content decrement?; ii) is Poisson coefficient an essential parameter in articular cartilage modeling?; iii) which phenomena, mechanical, chemical or electrical do manage tissue behavior?; (iv) are they combined to control tissue behavior or one of them is more relevant?

To solve these questions a previous developed three-dimensional mechano-electrochemical model (Manzano et al. 2014a; Manzano et al. 2014 b) has been used to analyze and quantify the influence of each parameter variation into cartilage behavior. Specifically, Young's modulus ( $E$ ), Poisson coefficient ( $\nu$ ), cation and anion diffusivities ( $D^+$  and  $D^-$  respectively), cation and anion activity coefficient ( $\gamma^+$  and  $\gamma^-$  respectively) changes have been addressed. To our knowledge, this is the first parametric study that determines the influence of these properties in an isolate manner in cartilage behavior, resulting in a basic guide to select the main parameters required for articular cartilage simulation. Note that the model includes essential biological phenomena, previously described in literature, that affect cartilage behaviour (diffusive-convective events and mechano-electrochemical effects) (Mow and Guo, 2002; Sun et al., 1999; Lai et al., 1991). However, it excludes those that experimentally show less influence as the viscosity of the solid matrix. Often, material models of articular cartilage exclude this effect since in short-term type of simulation the viscosity does not play a great role and articular cartilage appears as an elastic

solid with lower compressibility (Argatov and Mishuris 2015; Julkunen et al., 2013). Results show that (i) only collagen degradation is required to promote tissue swelling; (ii) minimal variation in  $\nu$  generates significant differences in tissue swelling and water and anion fluxes; (iii) variation in  $D^+$  and  $D^-$  seems to have less influence in capturing cartilage behavior than the mechanical parameters, however, they control the velocity of ion fluxes and finally, (iv) similar to  $D^+$  and  $D^-$ ,  $\gamma^+$  and  $\gamma^-$  show lower influence into tissue deformation (one order or magnitude less) than the studied mechanical properties.

The presented parametric study is a helpful tool to decipher the effects on cartilage simulated behaviour when varying Young's modulus, Poisson coefficient, and ion activity and diffusivity coefficients. Besides, the inclusion of repulsion phenomenon due to negative fixed charges attached to proteoglycans and the 3D nature of the model, present this algorithm as a new and easy method for the analysis and selection of the main parameters to include in cartilage computational models.

## **2 Material and methods**

Based on our previous work (Manzano et al. 2014a) four phases are considered: negatively charged porous-elastic solid (s), fluid (f), cations (+) and anions (-). These phases dynamically interact with each other triggering essential mechano-electrochemical phenomena for cartilage maintenance (for more details see (Sun et al. 2004; Manzano et al. 2014a; Manzano et al. 2014b)).

## 2.1 Mechano-electrochemical model

### 2.1.1 Governing equations

The governing equations of the model are based in the momentum and mass balance for the whole mixture and the charge balance for each ion. The relation between the four basic unknowns ( $\mathbf{u}^s$  the displacement of the solid matrix,  $\varepsilon^w$  the chemical potential of water,  $\varepsilon^+$  and  $\varepsilon^-$  the electrochemical potentials for cations and anions respectively) are summarized below,

*Momentum balance equation for the whole mixture*

$$\nabla \cdot \underbrace{\boldsymbol{\sigma}}_{\boldsymbol{\sigma}^f + \boldsymbol{\sigma}^c + \boldsymbol{\sigma}^s} = \mathbf{0}. \quad (1)$$

*Mass balance equation for the whole mixture*

$$\nabla \cdot \mathbf{v}^s + \nabla \cdot \mathbf{J}^w = 0. \quad (2)$$

*Charge balance equation for each studied ion*

$$\frac{\partial(\Phi^w c^+)}{\partial t} + \nabla \cdot \underbrace{\mathbf{J}^+}_{diffusion} + \nabla \cdot (\underbrace{\Phi^w c^+ \mathbf{v}^s}_{convection}) = 0, \quad (3)$$

$$\frac{\partial(\Phi^w c^-)}{\partial t} + \nabla \cdot \underbrace{\mathbf{J}^-}_{diffusion} + \nabla \cdot (\underbrace{\Phi^w c^- \mathbf{v}^s}_{convection}) = 0. \quad (4)$$

In these equations,  $\boldsymbol{\sigma}$  corresponds to the stress tensor related to the total mixture while  $\boldsymbol{\sigma}^f$ ,  $\boldsymbol{\sigma}^c$  and  $\boldsymbol{\sigma}^s$  are the stress tensors of the fluid, chemical and solid phases respectively.  $\mathbf{v}^s = \frac{\partial \mathbf{u}^s}{\partial t}$  refers to the velocity of the solid matrix. Note that in equation 1, body and inertial forces are neglected. Moreover, small strain formulation is adopted. Besides,  $c^+$  and  $c^-$  are cation and anion concentrations respectively. Finally,  $\Phi^w$  corresponds to the porosity of the tissue (Sun et al. 2004). Regarding the different

fluxes, the water flux,  $\mathbf{J}^w$ , cation flux,  $\mathbf{J}^+$ , and anion flux,  $\mathbf{J}^-$ , can be written as a combination of the electrochemical potentials,

$$\mathbf{J}^w = -\frac{R T \Phi^w}{\alpha} \left( \nabla \varepsilon^w + \frac{c^+}{\varepsilon^+} \nabla \varepsilon^+ + \frac{c^-}{\varepsilon^-} \nabla \varepsilon^- \right), \quad (5)$$

$$\mathbf{J}^+ = -\frac{R T \Phi^w c^+}{\alpha} \nabla \varepsilon^w - \left[ \frac{\Phi^w c^+ D^+}{\varepsilon^+} + \frac{R T \Phi^w (c^+)^2}{\alpha \varepsilon^+} \right] \nabla \varepsilon^+ - \frac{R T \Phi^w c^+ c^-}{\alpha \varepsilon^+} \nabla \varepsilon^-, \quad (6)$$

$$\mathbf{J}^- = -\frac{R T \Phi^w c^-}{\alpha} \nabla \varepsilon^w - \left[ \frac{\Phi^w c^- D^-}{\varepsilon^-} + \frac{R T \Phi^w (c^-)^2}{\alpha \varepsilon^-} \right] \nabla \varepsilon^- - \frac{R T \Phi^w c^+ c^-}{\alpha \varepsilon^+} \nabla \varepsilon^+, \quad (7)$$

Here,  $\alpha$  refers to the drag coefficient between the solid and the water phases. Atmospheric conditions are assumed where  $R$  is the universal gas constant and  $T$  is the absolute temperature (Garcia and Cortes 2006). The corresponding constitutive equations associated to the state variables, referring to equations 1-7, are also given by,

$$\boldsymbol{\sigma} = \underbrace{\frac{-P \mathbf{I}}{\sigma^f}}_{\text{osmotic pressure}} + \underbrace{\frac{-T_c \mathbf{I}}{\sigma^c}}_{\text{PGs repulsion}} + \underbrace{\frac{+\lambda_s \theta \mathbf{I} + 2\mu_s \boldsymbol{\epsilon}}{\sigma^s}}_{\text{elastic stress}}, \quad (8)$$

$$\varepsilon^w = \frac{P}{R T} - \Phi(c^+ + c^-) + \frac{B_w}{R T} \theta, \quad (9)$$

$$\varepsilon^+ = \gamma^+ c^+ \exp\left(\frac{F_c \psi}{R T}\right), \quad (10)$$

$$\varepsilon^- = \gamma^- c^- \exp\left(-\frac{F_c \psi}{R T}\right), \quad (11)$$

where  $\psi$  is the electrical potential,  $B_w$  is the fluid-solid coupling coefficient,  $F_c$  is the Faraday constant,  $\Phi$  is the osmotic coefficient, and  $\mathbf{I}$  is the identity tensor. Here,  $P$

refers to the fluid pressure,  $\theta = \text{div } \mathbf{u}^s$  corresponds to the solid matrix dilatation related to the infinitesimal strain tensor of the solid matrix,  $\epsilon$  is the solid matrix deformation, and finally,  $\lambda_s$  and  $\mu_s$  are the Lamé constants (Garcia and Cortes 2006). The chemical expansion due to proteoglycan repulsion phenomenon,  $T_c$ , is considered into the computational model though the following constitutive equation.

$$T_c = a_0 c^F \exp\left(-k \frac{\gamma^{\mp}}{\gamma^{\mp*}}\right) \sqrt{c(c + c^F)}.$$

Here, where  $a_0$  and  $k$  are the proteoglycan repulsion coefficients.  $\gamma^{\mp}$  and  $\gamma^{\mp*}$  are the mean activity coefficient of ions along the process and in the reference state, respectively.  $c$  refers to the neutral external salt concentration (Manzano et al. 2014b; Lai et al. 1991).

Tissue anisotropy has been mathematically incorporated though the depth-dependent distribution of fixed charges attached to proteoglycans, porosity and ion concentrations within the tissue (Manzano et al. 2014a; Manzano et al. 2014b).

### 2.1.2 Numerical implementation

Three-linear 8-noded hexahedral elements with 2×2×2 Gaussian integration points are used. The selected average mesh results in a total of 1680 elements. The highly non-linear finite element formulation has been implemented in a user defined element subroutine of the commercial software package Abaqus 6.11. A detailed description of the discretization developed for the formulation is collected in the previous work (Manzano et al. 2014a).



## 2.2 Numerical application

The geometry reproduced as well as the experimental procedure corresponds to those assays described by Lai et al. (1991). Therefore, this experimental situation is computationally reproduced to analyze and monitor the effect of mechano-electrochemical parameters in cartilage behavior (Figure 1). Dimensions of cartilage specimen correspond to 1.5 mm diameter and 0.5 mm depth and the sample is fixed in a confining ring where the z-displacement of the sample is free. Under these conditions, external bath solution is modified from 0.15 M to 0.125 M to reach similar cartilage swelling observed in physiological conditions. No loads are applied onto the sample in z-direction. The ranges of the studied parameters variation are, Young's modulus (from 0.35 to 1 MPa), Poisson coefficient (from 0.12 to 0.36), ion diffusivities ( $0.79 \cdot 10^{-9}$  to  $1.65 \cdot 10^{-9}$  m<sup>2</sup>/s) and/or ion activity coefficients (from 0.527 to 0.72), while the rest of model parameters included into the computational model are fixed (Table 1). Accurate quantification of ion fluxes within the samples and motorization of tissue changes along the swelling processes are obtained.

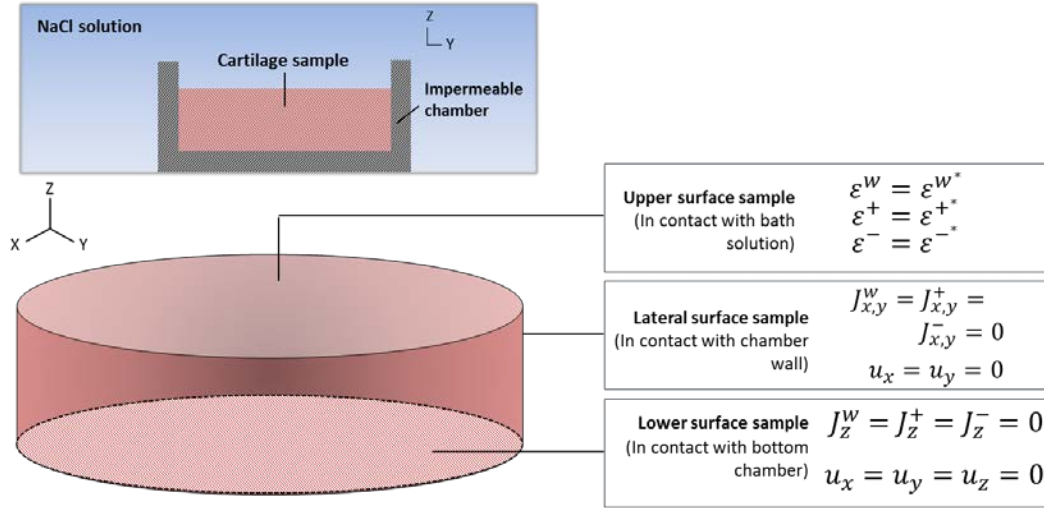


**Figure 1:** Schematic representation of the cartilage sample immersed in NaCl solution with an initial concentration of 0.15 M. Boundary conditions of the cartilage sample applied in the computational simulation developed for the parametric study.

### 2.2.1 Boundary conditions

Boundary conditions of the sample have been established in accordance to confined conditions planned experimentally (see Figure 1),

*Free surface:*

$$\sigma_z = 0; \quad \varepsilon^w = \varepsilon^{w*}; \quad \varepsilon^+ = \varepsilon^{+*}; \quad \varepsilon^- = \varepsilon^{-*}.$$

*Lateral surface:*

$$u_x = u_y = 0; \quad J_{x,y}^w = J_{x,y}^+ = J_{x,y}^- = 0.$$

*Lower surface:*

$$\mathbf{u} = \mathbf{0}; \quad J_z^w = J_z^+ = J_z^- = 0.$$

At the beginning of the simulation,  $t = 0$  seconds, the concentration of the external solution,  $c^*$ , is changed as occurs physiologically, from 0.15 M to 0.125 M. Then, the tissue response is analyzed from the results of the model described above. In these equations, superscript  $*$  stands for the quantities in the bath solution. It is important to note that the reduced diameter of the sample, 1.5 mm, make that not only  $u_z$  will be constrained in the lower area of the sample, but also  $u_x$  and  $u_y$ . Both will be null due to the constriction caused by the rigid and impermeable ring extended to the inner area of the sample.

### 2.2.2 Initial conditions

The cartilage sample is initially equilibrated with NaCl bath solution, with concentration of  $c^*$ . At  $t = 0$  seconds, the conditions imposed for the cartilage sample are,

$$\mathbf{u} = \mathbf{0}; \quad \varepsilon^w = \varepsilon^{w*}; \quad \varepsilon^+ = \varepsilon^{+*}; \quad \varepsilon^- = \varepsilon^{-*},$$

The reference state selected for this problem refers to that where the tissue is in equilibrium with the bathing solution (time 0 seconds, undeformed configuration).

### 2.3 Mechano-electrochemical parameters

To fully understand the effect of mechano-electrochemical parameter variations in articular cartilage behavior, two groups of properties have been introduced in the computational model. The first, related to mechanical properties, such as  $E$  and  $\nu$  and the second one, the electrochemical properties,  $D^+$ ,  $D^-$ ,  $\gamma^+$  and  $\gamma^-$ .

Afterward, all these properties are varied in an individual manner to analyze and quantify their effect in cartilage simulated response. Note that the selected range for

each parameter corresponds to typical values reported in literature for articular cartilage simulations. Thus,  $E$  and  $\nu$  studied values have been extracted from literature related to mechanical aspects of cartilage (Manzano et al. 2014a; Sun et al. 1999; Wong et al. 2000); while electrochemical properties have been obtained from previous works related to the measure of these related properties (Sun et al. 1999; Filidoro et al. 2005; Deng et al. 2007).

### **3 Results and discussion**

#### **3.1 Analysis of the effect of the mechanical parameters in free cartilage swelling**

To fully understand the effect of mechanical properties variation, specifically,  $E$  and  $\nu$ , in articular cartilage behavior, these tissue properties have been ranged to their minimum to maximal value reported in literature. Thus, this range includes healthy and degenerated articular cartilage. They were introduced into previously developed three-dimensional computational models. Simulation results show how swelling of samples increases according to the reduction of  $E$  and  $\nu$ . Consistently, incoming water fluxes resulted higher to those samples with lower  $E$  and  $\nu$ . Regarding ion fluxes, higher values are obtained when increasing the mechanical properties of the tissue.

##### **3.1.1 Effects of Young's modulus variation**

###### *z-displacement*

When using a low matrix stiffness ( $E=1.0$  MPa and  $E=0.9$  MPa), the model displays a maximal displacement of  $7.05 \cdot 10^{-9}$  m and  $1.12 \cdot 10^{-8}$  m respectively, within 200 seconds of simulated time; subsequently after reaching its maximum value of  $z$ -displacement, the tissue swelling keeps constant until the end of the simulation, 3600 seconds. Note

that results are shown for 500 seconds of simulation to capture more in detail the saturated phase, corresponding to the process of massive entrance of fluid to the sample. After this phase, the equilibrium is reached and the volume of the sample keeps constant (Figure 2.a). For higher values of  $E$  ( $E=0.6$  MPa and  $E=0.35$  MPa), the results present higher z-displacement ranging from  $2.98 \cdot 10^{-7}$  m to  $1.41 \cdot 10^{-5}$  m after 1200 s and 800 s of simulated time respectively. The rest of parameters included into the computational model are collected in Table 1. Thus, it is observed that when  $E$  decreases, swelling increases in the tissue. It is important to note that this collagen deterioration and subsequent loss of matrix stiffness corresponds to those tissues with medium and advanced grades of degeneration such as in case of osteoarthritis and aged degenerated tissue. Thus, lower values indicate that the articular cartilage is in a healthy state and the rigidity of the collagen network is able to prevent the tissue to swell.

Description	Symbol	Range or studied value
Young's modulus	$E$	0.35 – 1.0 MPa
Poisson coefficient	$\nu$	0.12 – 0.36
Drag coefficient between the solid and the water phase	$\alpha$	$7 \cdot 10^{14}$ N·s·m <sup>-4</sup>
Diffusivity of the cations	$D^+$	$0.79 \cdot 10^{-9} - 1.65 \cdot 10^{-9}$ m·s <sup>-1</sup>
Diffusivity of the anions	$D^-$	$0.79 \cdot 10^{-9} - 1.65 \cdot 10^{-9}$ m·s <sup>-1</sup>
Initial FCD	$c_0^F$	0.2 mEq·ml <sup>-1</sup>
Activity coefficient of cations	$\gamma^+$	0.527 – 0.72
Activity coefficient of anions	$\gamma^-$	0.695 – 0.72
Gas constant	$R$	8.314 J·mol <sup>-1</sup> ·K <sup>-1</sup>
Absolute temperature	$T$	298 K
Osmotic coefficient	$\Phi$	0.8
Initial amount of water in the tissue	$\Phi_0^w$	0.75

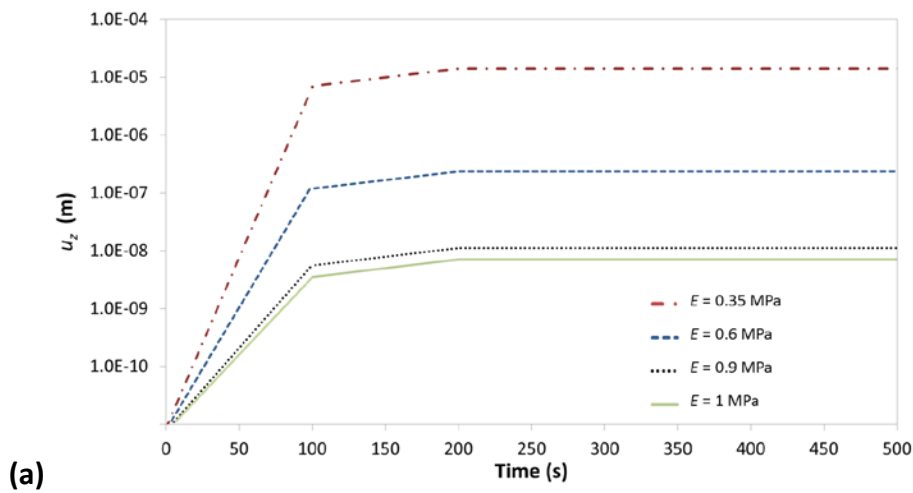
**Table 1:** Model parameters used in the 3D computational model to simulate articular cartilage swelling extracted from the previously developed model (Manzano et al. 2014a; Manzano et al. 2014b)

### *Water and ion fluxes*

The influence of  $E$  variation in water and ion fluxes is also considered. Simulation results are shown for maximal and minimum tissue stiffness after 200 seconds of simulated swelling, coincident with the period of maximal water entrance. Results demonstrate that, similarly to swelling, variation of  $E$  produces important alterations in water and ion fluxes. As explained in previous section, external bath is diluted to 0.125 M of NaCl resulting in an imbalance between inside of the tissue and the external solution. Hence, for the lower stiffness of the tissue,  $E=0.6$  MPa, values of water fluxes exhibit a maximum at the upper surface of the sample correspondent to  $1.54 \cdot 10^{-9}$  m<sup>3</sup>/s. This value is gradually decreased toward the lower surface of the sample. The same tendency is observed for higher values of tissue stiffness,  $E=1.0$  MPa, however, the incoming water flux is significantly reduced in this case, being their maximum value equal to  $5.47 \cdot 10^{-10}$  m<sup>3</sup>/s at the upper surface. Note that water and ion fluxes represented for each mechano-electrochemical parameter refer to the net flux of each species (water, cation and ion) where the influence of the flux in each direction is considered. Biologically, when collagen structure suffers a deterioration due to any cartilage disease,  $E$  is reduced, the capacity of the collagen network to retain water decreases and its ability to prevent cartilage swelling is also reduced (Figure 2.b). Note that water content is essentially controlled by the porosity of the tissue. The influence of this parameter into tissue swelling was analysed in our previous work in an isolated manner as well as the osmotic coefficient and the fixed charge density variation effects (Manzano et al. 2014a).

Importantly, here the effect of  $E$  variation is done as an isolated event, and not in combination with proteoglycans decrement or other related phenomena, to analyze its effects in tissue swelling. This fact confirms that the collagen degradation is essential to promote tissue swelling.

Regarding ion fluxes, both anions and cations reached their maximum value for higher  $E$  value ( $E=1.0$  MPa), ranging from  $-5.10 \cdot 10^{-5}$  mol/s (at the lower surface of the sample) to  $-4.40 \cdot 10^{-4}$  mol/s (at the upper surface of the sample) in case of cation fluxes while  $-2.77 \cdot 10^{-5}$  mol/s (at the bottom surface of the sample) to  $-4.79 \cdot 10^{-4}$  mol/s (at the upper surface of the sample) in case of anion fluxes. When  $E$  decreases, this pattern is altered and lower fluxes of anions occur; from  $-5.10 \cdot 10^{-5}$  mol/s (at the bottom surface of the sample) to  $-9.42 \cdot 10^{-5}$  mol/s (at the upper surface of the sample) in case of cation fluxes and  $-2.77 \cdot 10^{-5}$  mol/s (at the bottom surface of the sample) to  $-7.27 \cdot 10^{-5}$  mol/s (at the upper surface of the sample) in case of anion fluxes. Thus, for lower stiffness of the tissue, cation and anion fluxes are clearly overpassed by the intake water flux, which leads to higher substrate swelling.



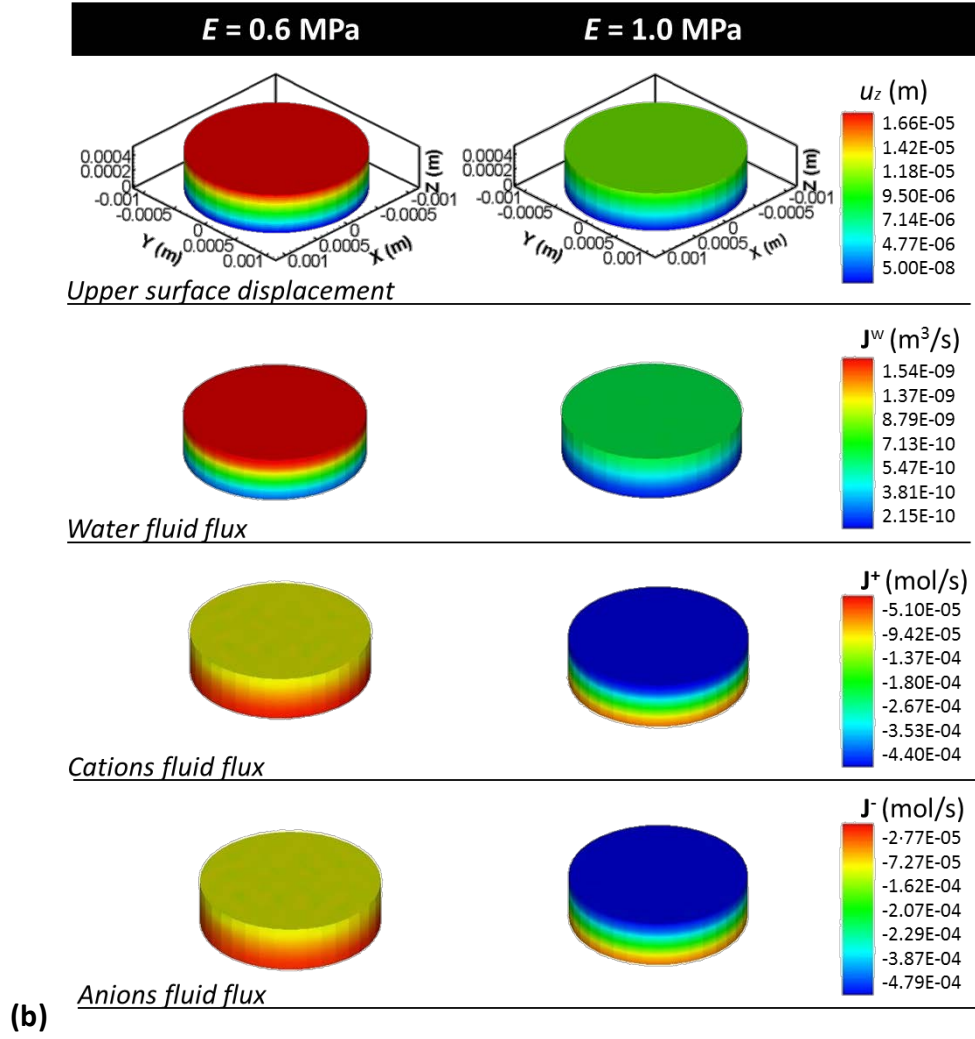


**Figure 2: (a)** Surface displacement obtained with the 3D computational model as function of the tissue Young's modulus ( $E$ ). The rest of model's parameters are included in Table 1. **(b)** Z-displacement ( $u_z$ ), water ( $J^w$ ), cation ( $J^+$ ) and ion ( $J^-$ ) fluxes obtained with the 3D computational model during 90 seconds of simulated time for  $E = 0.6$  MPa and  $E = 1.0$  MPa. Note that negative fluxes for each studied species correspond to the emergence of that component from the sample to the external bath. Conversely, positive fluxes refer to the entrance of the different components (water or ions) into the sample (tissue gain of material). Rest of parameters included in Table 1.



### 3.1.2 Effects of Poisson coefficient variation

#### *z-displacement*

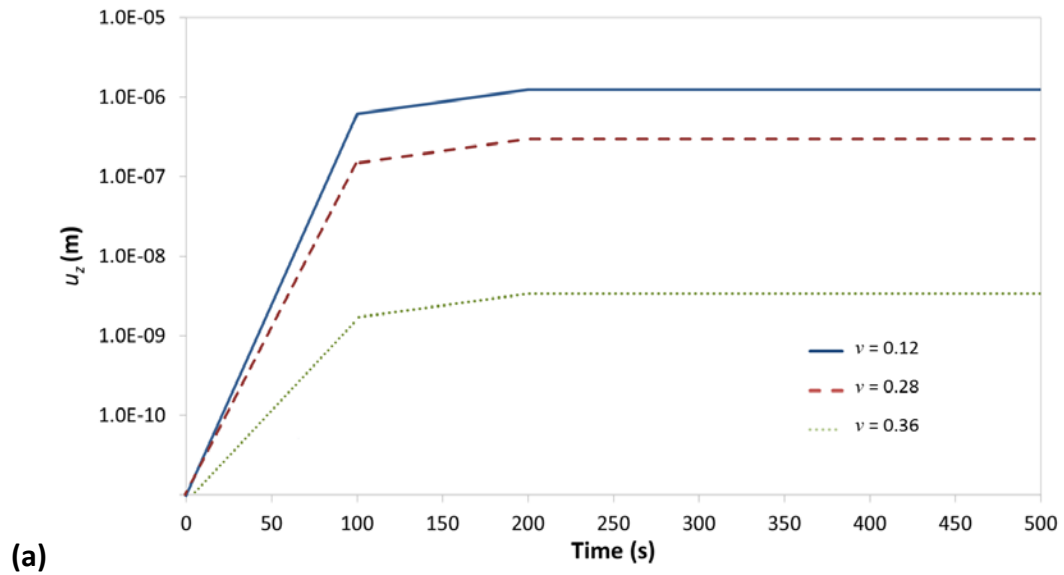
To study  $\nu$  the three most used values for articular cartilage modeling have been analyzed. For  $\nu = 0.36$ , simulation results showed a maximal  $z$ -displacement of  $9.45 \cdot 10^{-4}$  m. When, the value of this parameter is reduced to  $\nu = 0.28$ , the displacement reaches a maximum value of  $3.04 \cdot 10^{-4}$  m (Figure 3.a). Despite of expecting an increment of tissue swelling when decreasing  $\nu$ , the difference between the three studied values show three orders of magnitude. Consistently,  $\nu$  seems to represent, in combination with  $E$ , an essential parameter to include and thus, its accurate determination is essential to also obtain accurate results in simulation. Importantly, increment in  $\nu$  is observed in osteoarthritic tissue even in the first stage of the disease (Pearle et al., 2005). Besides this increase in the tissue rigidity is also shown in aged articular cartilage (Bhosale et al., 2008).

#### *Water and ion fluxes*

Interestingly, water and ion fluxes showed even higher influence in morphological changes of the samples than  $E$  since they also control the stiffness of the tissue in an indirect manner. Thus, according to experimental measures, the physiological values commonly used in computational simulation of articular cartilages are  $\nu = 0.28$  and  $\nu = 0.36$ . Both values have been considered in the present computational model resulting into significant differences in the simulated swelling process. For  $\nu = 0.28$  the incoming water flux goes from  $5 \cdot 10^{-8}$  m<sup>3</sup>/s (at the lower surface of the sample) to  $6.37 \cdot 10^{-7}$  m<sup>3</sup>/s (at the upper surface of the sample) (Figure 3.b). Note that, as explained before, these values are one order of magnitude higher than the water fluxes obtained with

previously studied  $E$  variation. Regarding ion fluxes, Figure 3.b shows how outgoing cation ranged from  $1.80 \cdot 10^{-5}$  mol/s to  $5.46 \cdot 10^{-5}$  mol/s while anion fluxes present a maximum of  $1.87 \cdot 10^{-5}$  mol/s at the upper surface and reduced to  $4.43 \cdot 10^{-5}$  mol/s at the bottom of the sample.

In contrast, when  $v$  is increased to 0.36, maximal water flux toward the external bath is reduced to  $3.76 \cdot 10^{-7}$  m<sup>3</sup>/s at the upper surface and the cation and anion fluxes exhibit a wide range from  $1.80 \cdot 10^{-5}$  mol/s to  $1.28 \cdot 10^{-4}$  mol/s.



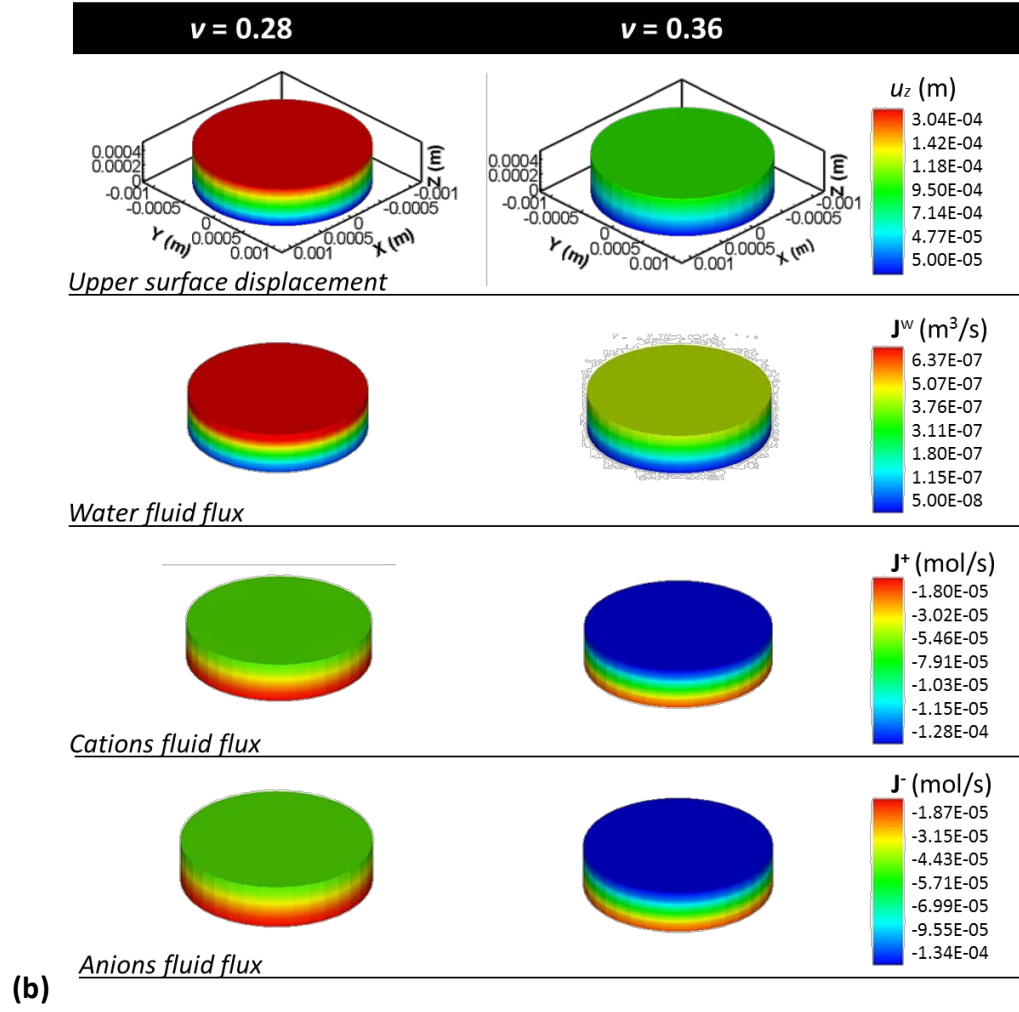


**Figure 3: (a)** Surface displacement obtained with the 3D computational model as function of the tissue Poisson coefficient ( $\nu$ ). The rest of model parameters are included in Table 1. **(b)** Z-displacement ( $u_z$ ), water ( $J^w$ ), cation ( $J^+$ ) and ion ( $J^-$ ) fluxes obtained with the 3D computational model during 90 seconds of simulated time for  $\nu = 0.28$  and  $\nu = 0.36$ . Note that negative fluxes for each studied species correspond to the emergence of that component from the sample to the external bath. Conversely, positive fluxes refer to the entrance of the different components (water or ions) into the sample (tissue gain of material). Rest of parameters included in Table 1.

### **3.2 Analysis of the effect of the electrochemical parameters in the free cartilage swelling**

In this study, the model has been also applied to analyze the effect of the main electrochemical parameters that affect cartilage behavior such as ion diffusivities and ion activity coefficients, since cartilage maintenance is based in mediated diffusive processes controlled by these parameters. Simulation results show a lower influence of these coefficients in comparison with those related to mechanical properties of the articular cartilage.

#### **3.2.1 Ion diffusivities**

Ion diffusivities control the flux velocity of cations and anions in the tissue when a gradient in ion concentrations is produced. As mentioned above, the external solution is diluted to 0.125 M NaCl which generates an imbalance between the inner and the outer medium of the sample.

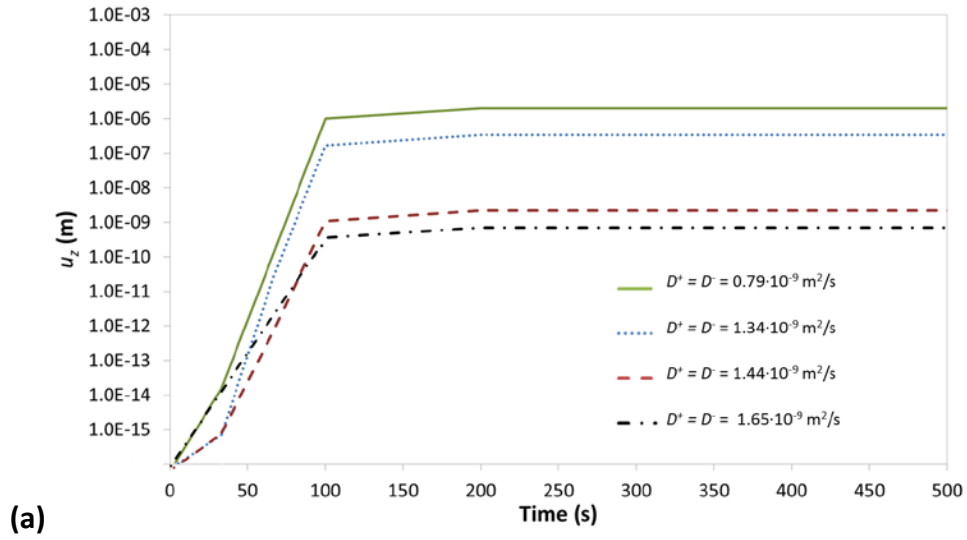
#### *z-displacement*

Physically, to balance of difference in ion concentration created between inside and outside of the tissue, two flows appear: (i) water incoming flow that causes swelling of the sample and (ii) outgoing ion flows. When ion diffusivity is high, the increment of the velocity in outgoing flux of ions produces that these ions flow toward the external bath to equilibrate the concentration disbalance. Thus, water entrance to the sample is reduced. Figure 4.a shows this tendency. When  $D^+ = D^- = 0.79 \cdot 10^{-9} \text{ m}^2/\text{s}$ , the maximal  $z$ -displacement obtained is  $1.99 \cdot 10^{-6} \text{ m}$ . When diffusivities are reduced, the model shows lower swelling of the sample reaching its minimum level at  $7.08 \cdot 10^{-10} \text{ m}$  for  $D^+ = D^- =$

$1.34 \cdot 10^{-9} \text{ m}^2/\text{s}$ . High values of ion diffusivity coefficients are related to different cartilage pathologies such as the osteoarthritis (Deng et al., 2007; Filidoro et al., 2005).

### *Water and ion fluxes*

Again water, cation and anion fluxes at 90 s are shown again. Three-dimensional computational simulation results show the typical flux pattern exhibited in previous studies. Samples clearly highlights the upper as the one with higher outflow zone of cations with  $J^+ = -7.83 \cdot 10^{-5} \text{ mol/s}$  and  $J^- = -8.90 \cdot 10^{-5} \text{ mol/s}$  for anions when considering lower values of  $D^+ = D^- = 1.34 \cdot 10^{-9} \text{ m}^2/\text{s}$ . When diffusivities are increased, simulations show how both cation and anion fluxes increase  $J^+ = -1.78 \cdot 10^{-5} \text{ mol/s}$  and  $J^- = -1.93 \cdot 10^{-5} \text{ mol/s}$  while outflow of water is reduced in the upper surface (Figure 4.b).



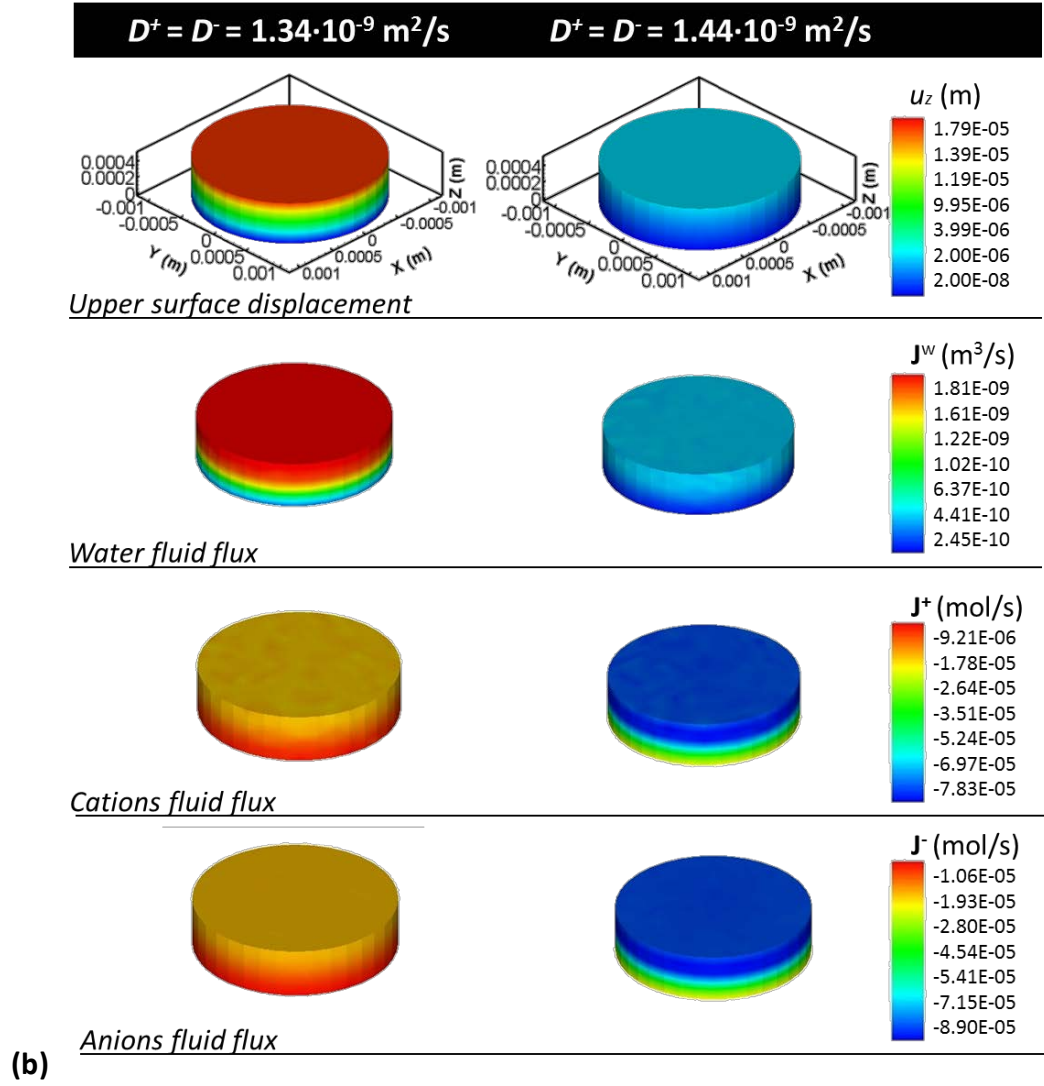


**Figure 4:** (a) Surface displacement obtained with the 3D computational model as function of the tissue ion diffusivity coefficients ( $D^+$ ,  $D^-$ ). The rest of model parameters are included in Table 1. (b) Z-displacement ( $u_z$ ), water ( $J^w$ ), cation ( $J^+$ ) and ion ( $J^-$ ) fluxes obtained with the 3D computational model during 90 seconds of simulated time for  $D^+ = D^- = 1.34 \cdot 10^{-9} \text{ m}^2/\text{s}$  and  $D^+ = D^- = 1.44 \cdot 10^{-9} \text{ m}^2/\text{s}$ . Note that negative fluxes for each studied species correspond to the emergence of that component from the sample to the external bath. Conversely, positive fluxes refer to the entrance of the different components (water or ions) into the sample (tissue gain of material). Rest of parameters included in Table 1.

### 3.2.2 Ion activity coefficients

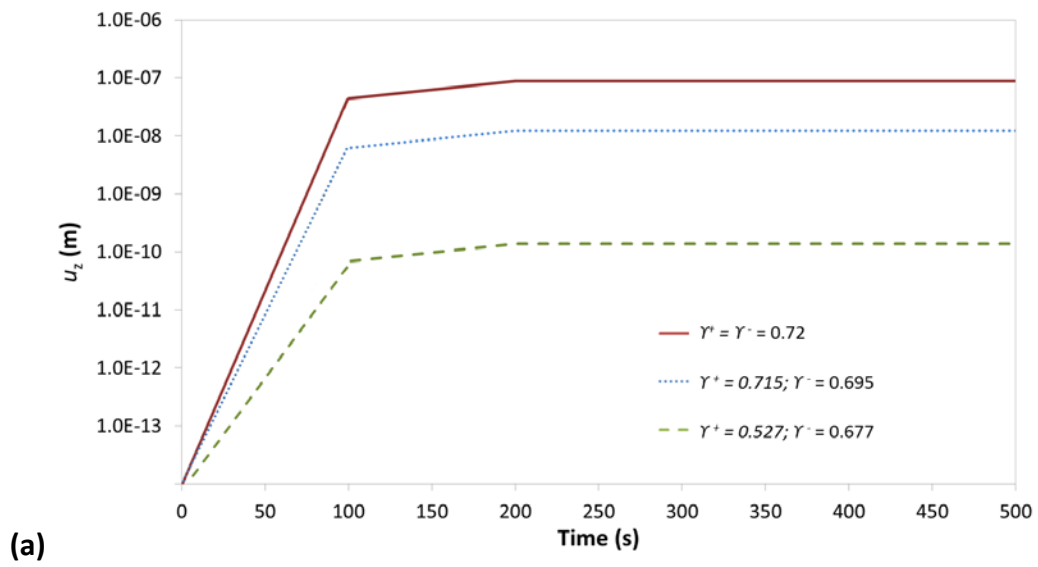
Finally, activity coefficients of cations and anions are also analyzed. Ion activity coefficients give a measure of the amount of ions that react in the solution. These parameters are of special interest in degenerative processes. Dai et al. in 1996 in their pioneer work demonstrated that in cartilage degenerative processes (Dai et al. 1996), where a sharp reduction of proteoglycans occurs and the subsequent decrement in fixed charge density, an increment in activity coefficient of ions was evidenced. Thus, in the present parametric study the effects of activities variation have been modelled to analyze its effect in articular cartilage behavior. Similar to ion diffusivity coefficients, high ion activity coefficients are commonly associated to cartilage pathologies such as osteoarthritis (Sun et al., 2004; Mow and Guo 2002; Sun et al., 1999).

#### *z-displacement*

Similar to diffusivity of ions, ion activity coefficients increase in case of cartilage degeneration. For high values of ion activity coefficients, the amount of ions that react inside the tissue is higher. Subsequently, the formation of salt generates higher disbalance between inside and outside the tissue. Then, the flux of water required to return the steady-state of the tissue is higher. So, simulation results show a maximal upper surface displacement of  $8.79 \cdot 10^{-8}$  m after 200 s of simulated time for  $\gamma^+ = \gamma^- = 0.72$  (see Figure 5.a). When this value decreases, swelling of the sample is significantly reduced. Anyhow, ion activity coefficients seem to have a lesser effect in cartilage behavior than the other parameters.

#### *Water and ion fluxes*

The influence of ion activity coefficients in water and ion fluxes has also been considered. Results demonstrate that, similar to diffusivity, higher values of  $\gamma^+$  and  $\gamma^-$  yield the highest water incoming flow,  $3.26 \cdot 10^{-9} \text{ m}^3/\text{s}$  and cation ( $J^+ = 5.50 \cdot 10^{-5} \text{ mol/s}$ ) and anion ( $J^- = 6.24 \cdot 10^{-5} \text{ mol/s}$ ) outflows. A slight reduction of all fluxes is evidenced when decreasing these ion activity coefficients as shown in Figure 5.b.





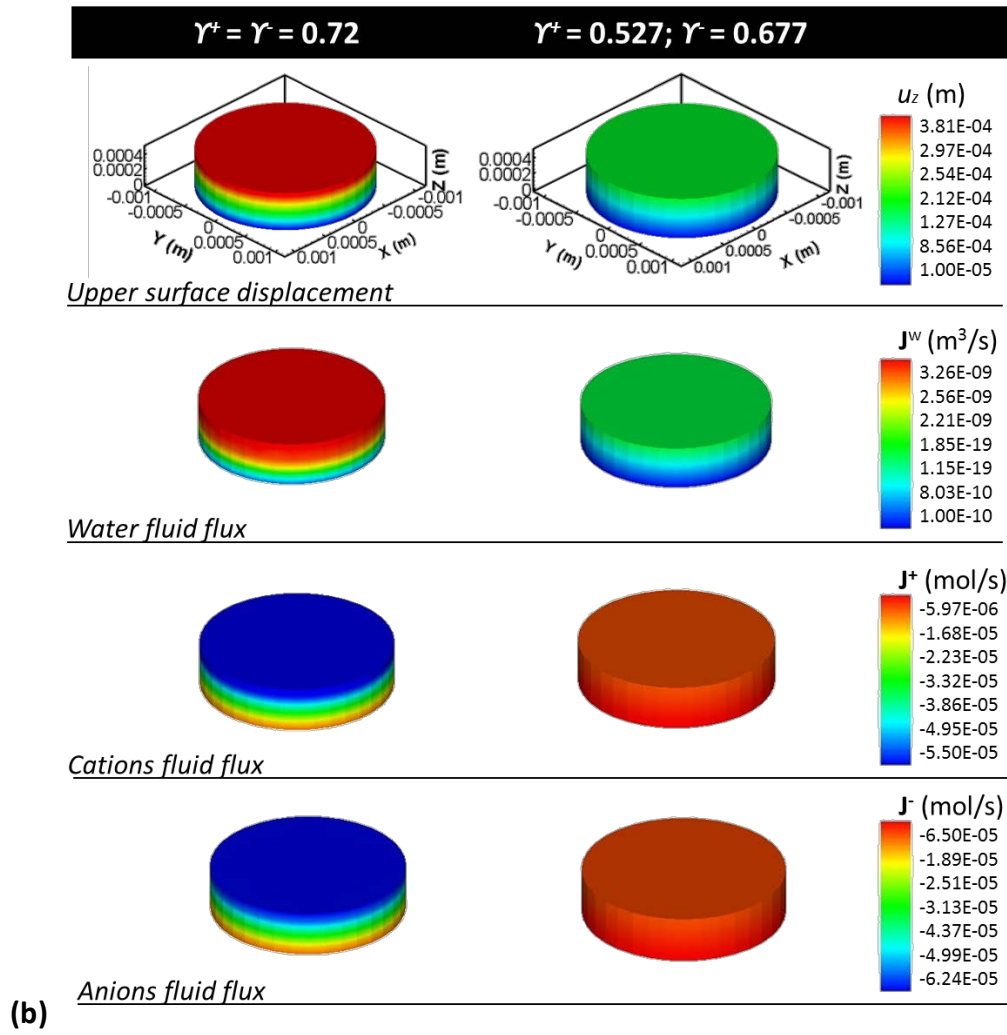


**Figure 5: (a)** Surface displacement obtained with the 3D computational model as function of the tissue ion activity coefficients ( $\gamma^+$ ,  $\gamma^-$ ). The rest of model parameters are included in Table 1. **(b)** Z-displacement ( $u_z$ ), water ( $J^w$ ), cation ( $J^+$ ) and ion ( $J^-$ ) fluxes obtained with the 3D computational model during 90 seconds of simulated time for  $\gamma^+ = \gamma^- = 0.72$  and  $\gamma^+ = 0.527; \gamma^- = 0.677$ . Note that negative fluxes for each studied species correspond to the emergence of that component from the sample to the external bath. Conversely, positive fluxes refer to the entrance of the different components (water or ions) into the sample (tissue gain of material). Rest of parameters included in Table 1.

## 4 Conclusions

In this work, a parametric study of the main mechano-electrochemical parameters of articular cartilage has been performed. To this aim, a previous developed three-dimensional mechano-electrochemical model has been used to analyze and quantify the influence of each parameter in cartilage behavior (Manzano et al. 2014a; Manzano et al. 2014b). Specifically,  $E$ ,  $\nu$ ,  $D^+$ ,  $D^-$ ,  $\gamma^+$  and  $\gamma^-$  effects have been addressed. To our knowledge, this is the first parametric study that determines the influence of these properties in an individual manner in cartilage behavior, resulting in a fundamental guide to select the main parameters required for articular cartilage simulation. The relevance of this previous validated model and its current application lies on the impossibility of setting up the parametric variation and subsequent analysis experimentally.

Under these conditions, the obtained results demonstrate that (i) only the consideration of collagen fibers degradation by reducing the  $E$  results in higher values of tissue swelling. Thus, in contrast with other authors that remark the necessity of including proteoglycan associated reduction, only collagen degradation is essential to promote tissue swelling. (ii) Regarding  $\nu$ , there is a general tendency to include this parameter in computational simulation as a constant and no experimental measurement is usually developed to determine its variation upon age, sex or part of the body where the tissue is found. However, results derived from this work showed that a minimal variation in  $\nu$  generates significant differences in tissue swelling and water and ion fluxes. Therefore, it is essential to include consistent values of  $\nu$  as well as its correlation with the rest of mechanical properties in computational simulation to

capture the correct articular cartilage behavior. Besides, both,  $E$  and  $\nu$ , have been shown to be the parameters with more influence in tissue behavior, among all studied properties. (iii) Variation in ion diffusivities seems to have less influence in cartilage behavior than the other mechanical parameters. In the other hand, they control the velocity of ion outgoing fluxes toward the external bath and limit the incoming flux of water. Thus, they also control swelling and tissue behavior but less than previously analyzed parameters. Finally, (iv) high values of ion activity coefficients generate higher disbalance between inside and outside the tissue, however, similar to ion diffusivities their influence is lower (one order or magnitude less) than the studied mechanical properties. Additionally, since articular cartilage behaviour has been evidenced to be very sensitive to variation of several mechano-electrochemical parameters, the use of additional sophisticated tools for parametric sensitivity analysis is suggested (Ramtani 2007; Raghavan and Vorp 2000). Their use could help in the better understanding of the involved parameters.

With all this, we consider that this parametric study represents a valuable tool to predict and quantify the impact of each mechano-electrochemical parameter into tissue deformation capacity.

## **Acknowledgements**

The authors gratefully acknowledge the financial support from the Spanish Ministry of Economy and Competitiveness (MINECO MAT2013-46467-C4-3-R and FPU graduate research programme AP2010/2557), the Government of Aragon (DGA) and CIBER-BBN

initiative. CIBER-BBN is financed by the Instituto de Salud Carlos III with assistance from the European Regional Development Fund.

### **Conflict of interest**

The authors declare that there is no conflict of interests regarding the publication of this paper.

### **References**

Albro MB, Rajan V, Li R, Hung CT, Ateshian GA. 2009. Characterization of the Concentration-Dependence of Solute Diffusivity and Partitioning in a Model Dextran-Agarose Transport System. *Cellular and molecular bioengineering* 2(3):295-305.

Argatov, I., Mishuris, G. 2015. *Contact Mechanics of Articular Cartilage Layers: Asymptotic Models*. Vol. 50. Springer.

Ateshian GA, Maas S, Weiss JA. 2013. Multiphasic Finite Element Framework for Modeling Hydrated Mixtures with Multiple Neutral and Charged Solutes. *Journal of Biomechanical Engineering* 135(11):011-111.

Bhosale, AM, Richardson, JB. 2008. Articular cartilage: structure, injuries and review of management. *British medical bulletin*, 87(1): 77-95.

Boschetti F, Pennati G, Gervaso F, Peretti GM, Dubini G. 2004. Biomechanical properties of human articular cartilage under compressive loads. *Biorheology* 41(3): 159-166.

Chen AC, Nguyen TT, Sah RL. 1997. Streaming potentials during the confined compression creep test of normal and proteoglycan-depleted cartilage. *Annals of Biomedical Engineering* 25(2): 269-277.

Dai H, Potter K, McFarland EW. 1996. Determination of ion activity coefficients and fixed charge density in cartilage with <sup>23</sup>Na magnetic resonance microscopy. *Journal of Chemical & Engineering Data*, 41(5), 970-976.

Deng X, Farley M, Nieminen MT, Gray M, Burstein D. 2007. Diffusion tensor imaging of native and degenerated human articular cartilage. *Magnetic Resonance Imaging*. 25(2): p. 168-71.

Filidoro L, Dietrich O, Weber J, Rauch E, Oerther T, Wick M, Reiser MF, Glaser C.. 2005. High-resolution diffusion tensor imaging of human patellar cartilage: feasibility and preliminary findings. *Magnetic Resonance Medicine*. 53(5): p. 993-8.

Garcia JJ and Cortes DH. 2006. A nonlinear biphasic viscohyperelastic model for articular cartilage. *Journal of Biomechanics* 39(16): p. 2991-8.

Higginson GR, Litchfield MR, Snaith J. 1976. Load-Displacement-Time Characteristics of Articular-Cartilage. *International Journal of Mechanical Sciences* 18(9): 481-486.

Julkunen, P., Wilson, W., Isaksson, H., Jurvelin, J. S., Herzog, W., Korhonen, R. K. 2013. A review of the combination of experimental measurements and fibril-reinforced modeling for investigation of articular cartilage and chondrocyte response to loading. *Computational and mathematical methods in medicine*, 2013.

Lai WM, Hou JS, Mow VC. 1991. A Triphasic Theory for the Swelling and Deformation Behaviors of Articular-Cartilage. *Journal of Biomechanical Engineering-Transactions of the Asme* 113(3): 245-258.

Manzano S, Gaffney EA, Doblare M, Doweidar MH. 2014a. Cartilage dysfunction in ALS patients as side effect of motion loss: 3D mechano-electrochemical computational model. *Biomed Research International*. Vol 2014.

Manzano S, Manzano R, Doblare M, Doweidar MH. 2014b. Altered swelling and ion fluxes in articular cartilage as a biomarker in osteoarthritis and joint immobilization: a computational analysis. *Journal of The Royal Society Interface* 12(102), 20141090.

Mow V, Guo XE. 2002. Mechano-electrochemical properties of articular cartilage: Their inhomogeneities and anisotropies. *Annual Review of Biomedical Engineering* 4(1): 175-209.

Pearle AD, Warren RF, Rodeo SA. 2005. Basic science of articular cartilage and osteoarthritis. *Clinics in sports medicine* 24(1): 1-12.

Smith DW, Gardiner BS, Davidson JB, Grodzinsky AJ. 2013. Computational model for the analysis of cartilage and cartilage tissue constructs. *Journal of tissue engineering and regenerative medicine*.

Landinez-Parra, N. S., Garzón-Alvarado, D. A., Vanegas-Acosta, J. C. 2011. A phenomenological mathematical model of the articular cartilage damage. *Computer methods and programs in biomedicine*, 104(3): 58-74.

Seifzadeh, A., Oguamanam, D. C. D., Trutiak, N., Hurtig, M., Papini, M. 2012. Determination of nonlinear fibre-reinforced biphasic poroviscoelastic constitutive

parameters of articular cartilage using stress relaxation indentation testing and an optimizing finite element analysis. *Computer methods and programs in biomedicine*, 107(2): 315-326.

Manzano, S., Poveda-Reyes, S., Ferrer, G. G., Ochoa, I., Doweidar, M. H. 2014. Computational analysis of cartilage implants based on an interpenetrated polymer network for tissue repairing. *Computer methods and programs in biomedicine* 116(3): 249-259.

Krishnan Namboori, P. K., Ranjini, U. P., A Manakadan, A., Jose, A., Silvipriya, K. S., Belzik, N., Deepak, O. M. 2013. Computational Modeling of Environmentally Responsive Hydrogels (ERH) for Drug Delivery System. *Current computer-aided drug design*, 9(1): 76-82.

Raghavan, M. L., Vorp, D. A. (2000). Toward a biomechanical tool to evaluate rupture potential of abdominal aortic aneurysm: identification of a finite strain constitutive model and evaluation of its applicability. *Journal of biomechanics*, 33(4): 475-482.

Ramtani, S. 2007. Parametric sensitivity analysis applied to a specific one-dimensional internal bone remodelling problem. *Computers in biology and medicine*, 37(8): 1203-1209.

Soulhat J, Buschmann MD, Shirazi-Adl A. 1999. A fibril-network-reinforced biphasic model of cartilage in unconfined compression. *Journal of Biomechanical Engineering-Transactions of the Asme* 121(3): 340-347.

Sun DD, Guo XE, Likhitanichkul M, Lai WM, Mow VC. 2004. The influence of the fixed negative charges on mechanical and electrical behaviors of articular cartilage under

unconfined compression. Journal of Biomechanical Engineering-Transactions of the Asme 126(1): 6-16.

Sun DN, Gu WY, Guo XE, Lai1 WM and Mow VC. 1999. A mixed finite element formulation of triphasic mechano-electrochemical theory for charged, hydrated biological soft tissues. International Journal for Numerical Methods in Engineering. 45(10): p. 1375-1402.

Virén T, Saarakkala S, Kaleva E, Nieminen HJ, Jurvelin JS, Töyräs J. 2009. Minimally Invasive Ultrasound Method for Intra-Articular Diagnostics of Cartilage Degeneration, Ultrasound in Medicine & Biology 35(9): 1546-1554.

Wilson W, van Donkelaar CC, van Rietbergen R, Huiskes R. 2005. The role of computational models in the search for the mechanical behavior and damage mechanisms of articular cartilage. Medical engineering & physics 27(10): 810-826.

Wong M, Ponticiello M, Kovanen V, Jurvelin JS. 2000. Volumetric changes of articular cartilage during stress relaxation in unconfined compression. Journal of Biomechanics. 33(9): 1049-54.